Lasers in Surgery and Medicine 21:294–300 (1997)

BRIEF REPORT

Dynamics of ArF Excimer Laser-induced Cavitation Bubbles in Gel Surrounded by a Liquid Medium

Daniel Palanker, PhD, Igor Turovets, PhD, and Aaron Lewis, PhD*

Laser Center, Hadassah Medical Organization and NanoMed, Jerusalem, Israel

Background and Objective: **Cavitation bubbles have been shown to be the driving force of tissue cutting in 193 nm ArF excimer laser-based vitreoretinal microsurgery. In the present work we investigate the dynamics of cavitation bubbles inside a gelatin gel in a saline environment using fast flash microphotography.** ***Study Design/Materials and Methods:*** **The screening influence of the saline medium was found to restrict the maximal distance between the tip and the tissue at which cavitation bubbles are created to <100 μm at an energy fluence up to 0.3 J/cm^2/pulse (the maximal energy fluence applied in vitreoretinal surgery).** ***Results and Conclusion:*** **Single laser pulses did not cause disruption of gelatin at an energy fluence of up to 0.4 J/cm^2/pulse. During the application of repetitive pulses small insoluble gas-containing bubbles were produced and often trapped between the tip and the tissue. They completely changed the shape of the subsequent cavitation bubbles and caused deep crater formation in the gel. Lasers Surg. Med. 21:294–300, 1997.**

Key words: cavitation bubble; vitreoretinal surgery; excimer laser; laser/tissue interaction; 193 nm

INTRODUCTION

Application of pulsed lasers for cutting or disruption of biological tissue in a liquid environment is generally associated with the appearance of cavitation bubbles. Such bubbles result from an explosive evaporation of water due to dielectric breakdown [1,2] or radiation absorption in water [3,4] or in tissue [5–7]. [1]These bubbles were found to be the main driving force of laser-assisted tissue cutting in a liquid environment [1,2,5,8–11]. Interaction of cavitation bubbles with tissue has been investigated in the case of dielectric breakdown generated by a laser beam tightly focused from outside the liquid medium in which tissue cutting occurs [2]. In the experiments with the fiber-delivered laser radiation, vapor bubbles have been observed above the tissue surface [5,6,12,13], but their geometry and dynamics as well as the associated deformations inside the tissue were observed only in the case of large (mm-size) cavitation bubbles created by the Ho:YAG laser inside the polyacrylamide gel [14].

We have applied the 193 nm ArF excimer laser to vitreoretinal surgery [7] and have demonstrated rapid cutting of retinal and membranous tissue in a liquid environment. Trying to explore the mechanism of this process, we simulated the tissue absorption by a highly absorbing liquid

[1]Re ref. 7: In order to calculate the energy fluence at the tip exit from this work one should multiply the exiting energy by a factor 0.55 and to divide it by the tip exit surface. This is in order to subtract the energy that exits through the walls of the tapered part of the tip, as it is described in Materials and Methods.

*Correspondence to: Aaron Lewis, Laser Center, Hadassah Medical Organization, P.O. Box 12000, Jerusalem 91120, Israel.

Accepted 10 October 1996

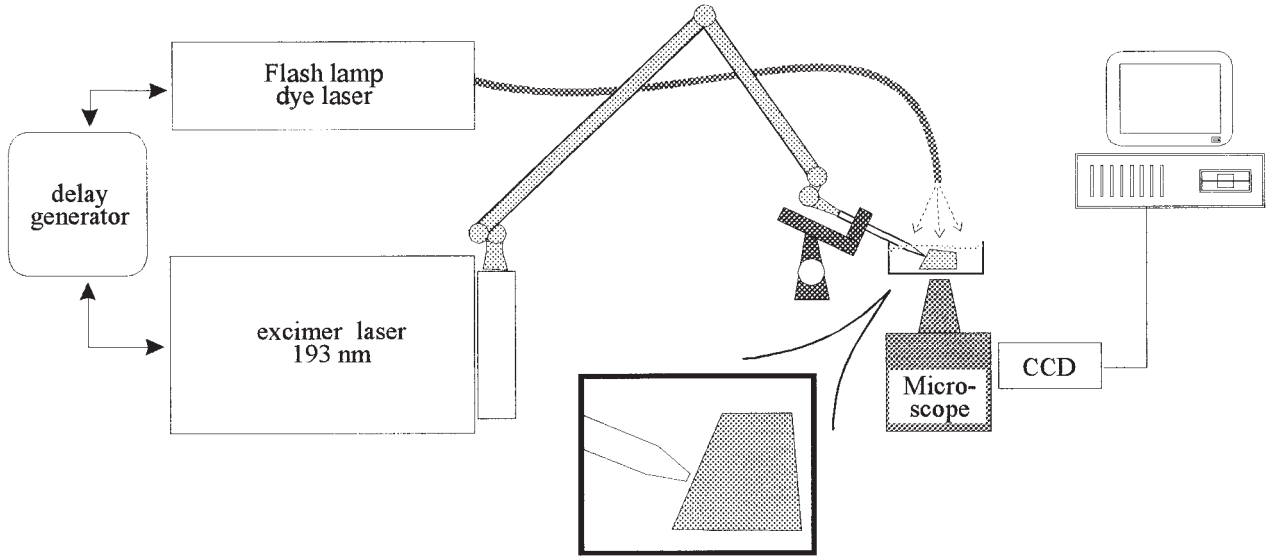

Fig. 1. Schematic representation of the experimental setup for fast micro photography.

medium (concentrated NaCl solution) and have observed generation of the cavitation bubbles using fast-flash photography [11]. In addition, during the irradiation of such solutions, insoluble bubbles consisting mainly of hydrogen gas have been detected [15].

For better understanding of the dynamics of cavitation bubbles inside tissue, we generate such bubbles in gelatin gel. This tissue model was chosen because the amino acid composition of gelatin is similar to that of collagen [16] and because such a gel is transparent to visible light. Thus the cavitation bubbles, the resulting material deformation and disruption easily can be observed inside this gel. In addition, we investigate in this work the influence of insoluble bubbles that result from ArF excimer laser irradiation on the cutting process. Finally, we determine the extent of the screening effect of the physiological medium that protects the underlying tissue.

MATERIALS AND METHODS

The experimental setup used for generation of cavitation bubbles with the ArF excimer laser and for the fast micrography was described elsewhere [11]. The laser pulse to pulse energy stability was within 10%. To decrease the uncertainty in the time delay of certain events of bubble dynamics as well as bubble dimensions, the frames were recorded only when the energy delivered through the tip differed by <1% from a preset value. The delay generator controlling the time delay between the pulses of the excimer and dye laser was calibrated using a photodiode (1 ns rise time).

Samples of 2-mm-thick gelatin gel of 20% w/v concentration were prepared by dissolving the required amount of gelatin (British Drug Houses, Pole, UK) in boiling distilled water with subsequent cooling. The samples were irradiated in a normal saline (9 g/L NaCl in water) environment.

The exit end of the optical fiber tip had a tapered shape schematically shown in Figure 1. The external diameter of the fiber was 1 mm with the cladding/core ratio 1.1. The exit diameters of the tips were in the range of 0.24–0.33 mm. The cone angle measured near the tip exit was 8 ± 1°. The laser power delivered through the tip was measured with a 03AP - DGX energy meter (Ophir, Jerusalem, Israel) at a repetition rate of 10 Hz. The radiation was concentrated inside the tapered area of the tip and partially exited through the walls. The energy E, exiting from the exit surface, varied in a range of 55–75% of the total energy transmitted through the tip, depending on the tip shape. This energy E was altered in the range of 0.03–0.3 mJ/pulse that corresponds to an average energy fluence at the exit surface varying in the range of 0.05–0.4 J/cm^2/pulse.

The ablating tip was held in a micromanipulator at an angle 18° with respect to the horizontal. The movements of the tip were accomplished with accuracy of +/− 5 μm. Prior to the irradiation, the front vertical side of each gelatin sample was cut at the same angle with respect to vertical,

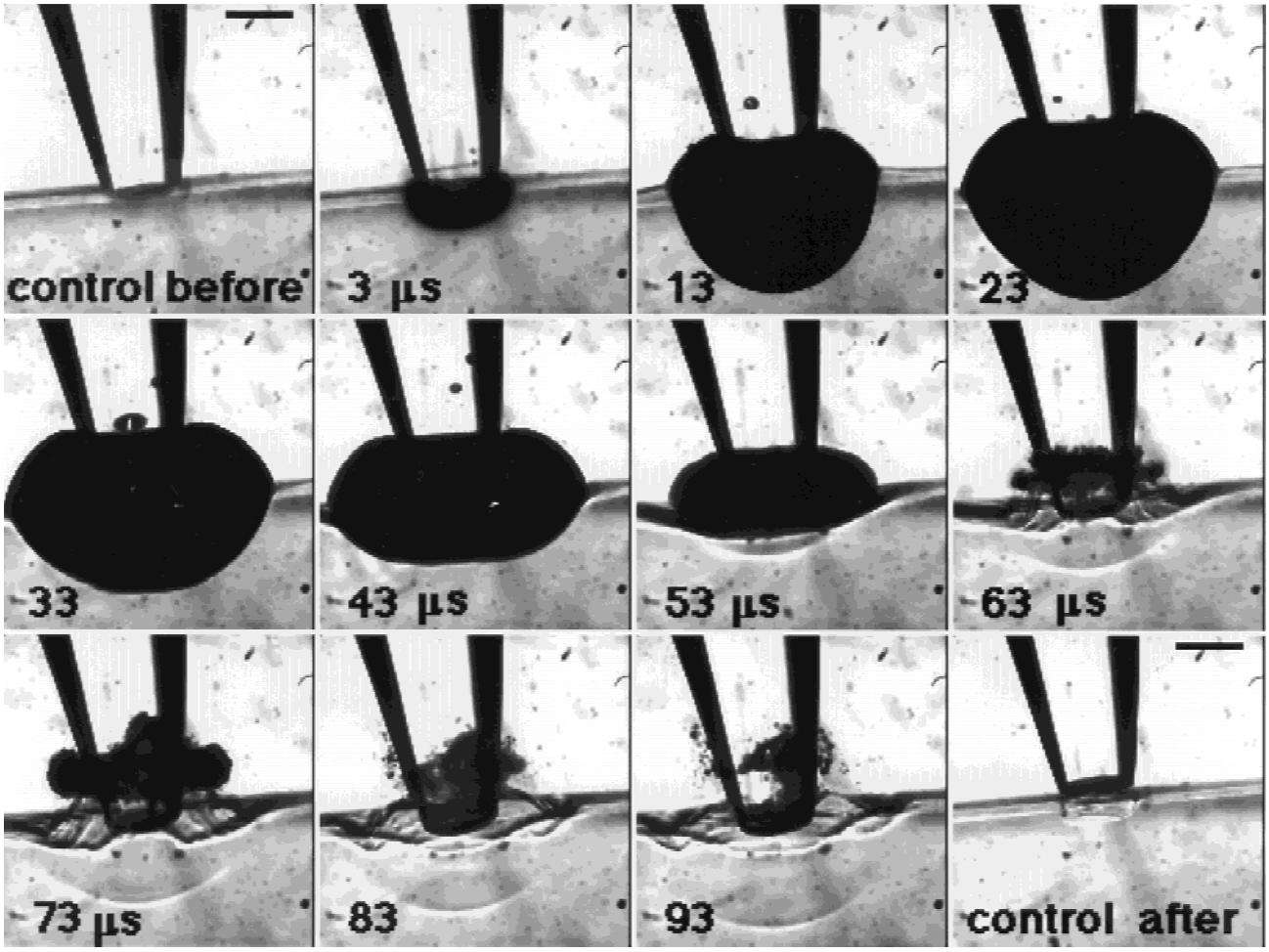

Fig. 2. Sequence of micrographs of cavitation bubble dynamics in gelatin gel. Fiber tip is in contact with the gelatin. Length of the bar is 0.25 mm. Laser energy fluence was 0.35 J/cm^2/pulse, tip exit diameter, 0.26 mm. Delay time in μs after the excimer laser pulse is shown in the corner of each frame.

so that the gelatin surface was perpendicular to the tip axis (see Fig. 1). The distance from the tip to a gel surface was varied in our experiments from contact conditions to 100 μm. Each pulse train was applied to the fresh untreated area. The time of irradiation of each sample was limited to 30 minutes because of the swelling of the gelatin.

RESULTS

Cavitation Bubble Dynamics

In Figure 2, a sequence of images presents the bubble kinetics in gelatin at an energy fluence of 0.35 J/cm^2/pulse and a tip exit diameter of 0.26 mm. During the growth phase, which lasted 25–30 μs, the bubble had a distorted sphere configuration with different radii of curvature inside and outside the gelatin. It penetrated inside to a depth of 430 μm 23 μs after the laser pulse. At 53 μs, a spherical wave of deformation in the gelatin appeared under the bubble and propagated with a velocity of 5.6 ± 0.2 m/s. Bubble collapse was observed at 63 ± 1 μs. After the collapse, a secondary ring-shape bubble was born around the tip above the material and moved away from the boundary (73 μs). The secondary bubble completely disappears 110 μs after the pulse. No disruption of the gel was detected after the application of a single laser pulse. The last frame of Figure 2 (labeled "Control After") shows a crater resulting from application of 20 pulses to the same point. (After each pulse the tip was withdrawn out of material and inserted back into contact with the gel in order to prevent accumulation of the insoluble gas between the tip and the sample.) The 80-μm-deep crater seen in this last frame of Figure 2 has a very accurate cylindrical shape with a flat bottom and a diameter equal to that of the tip. This crater

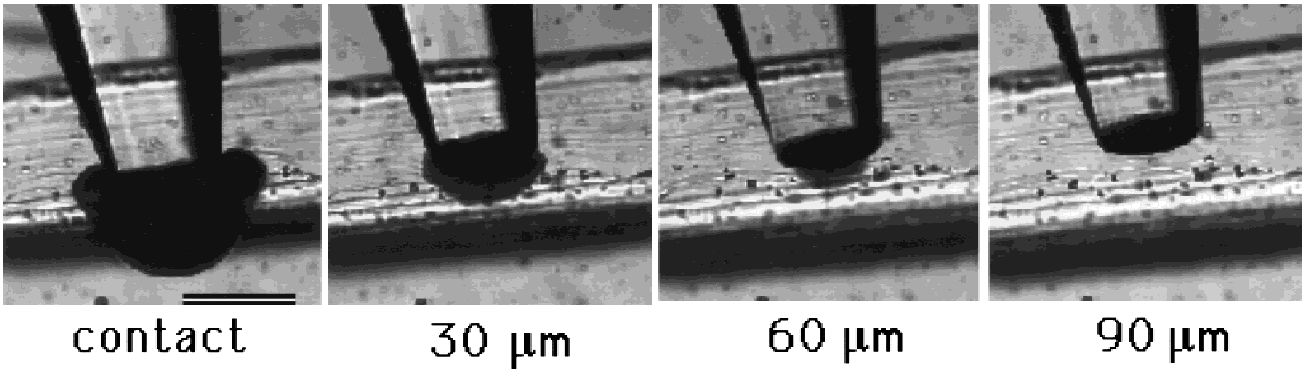

Fig. 3. Micrographs of cavitation bubbles at the maximal expansion stage at the different distances between the tip and the gelatin surface in normal saline medium. Length of the bar is 0.25 mm. Laser energy fluence was 0.15 J/cm^2/pulse, tip exit diameter, 0.24 mm. Distance between the tip and the surface in microns is shown under each frame. Delay time was 15 μs, 5 μs, 2 μs, and 1 μs in the frames (from left to right), respectively.

was deepened from pulse to pulse, and it seems that the process underlying the crater formation is mainly a photothermolysis of gelatin due to a heating in front of the tip.

At lower laser energy fluences, all processes following the laser irradiation of the gel become shorter and less profound. At an energy fluence of 0.15 J/cm^2/pulse, that corresponds to a total transmitted energy of 0.12 mJ/pulse—this is the medium energy that has been applied to vitreoretinal surgery [7]—the bubble grows for a shorter time ~15–20 μs and collapses at 30 ± 1 μs after the pulse. The maximal penetration of the bubble inside the gel is 150 μm. No ring formation and no deformation waves were observed after the bubble collapse.

Bubble dynamics was also investigated as a function of distance between the tip and the gel surface at this same energy fluence—0.15 J/cm^2/pulse. The maximal diameter of the bubble was determined at each distance in a series of experiments. The results are shown in Figure 3, where the distance (in μm) between the tip and the surface is presented under each frame. At 30 μm only a small vapor bubble (with the same diameter as the tip) is observed. (Due to the observation of this process at an angle, as shown in Figure 1, there is an illusion that bubbles grow from the tip and not from the gel surface.) The threshold distance of bubble appearance was ~60 μm, where just a minor opacity was observed between the tip and the gel.

Cavitation Bubble Dynamics in Presence of Insoluble Gas Bubbles

During the 193 nm excimer laser irradiation of saline and other liquid media containing chloride anions, the insoluble bubbles containing hydrogen gas are generated due to water decomposition [15]. In the case of irradiation of biological tissue, these bubbles also can contain the volatile products of tissue decomposition. When the fiber tip was slightly pressing against the gelatin during the irradiation, such small insoluble bubbles—with a diameter varying in a range of 50–80 μm—were sometimes confined between the tip and the sample. They dramatically changed the dynamics and the shape of the cavitation bubble generated in the sample by the next laser pulse. As a result, instead of a shallow hole with a diameter equal to the diameter of the tip that was produced in the gel after each pulse in a single pulse experiment, a deep narrow crater was created after application of a pulse train. An example of such a crater of ~70 μm in width and 170 μm in depth obtained at an energy fluence of 0.35 J/cm^2/pulse is shown in frame 3, Figure 4A. It was created due to interaction of the confined insoluble bubble of ~70 μm in diameter created after the first laser pulse, with the vapor bubble generated after the second laser pulse. The resulting process looks like as if a small gas ball (see arrow in Fig. 4B, frame 2) is pushed into the gel by a cavitation bubble producing a narrow hole (Fig. 4B, frame 3) with the same diameter as that of the insoluble bubble. The shape of the cavitation bubble in the presence of the gas bubble differs from the bubble produced in the absence of a previously produced insoluble bubble. In Figure 4C, frame 1, a crater is shown that had a stepped shape and was filled with gas before the laser pulse. The vapor bubble inflated the gas filled volume to the maximal expansion shown in frame 2. This eventually cre-

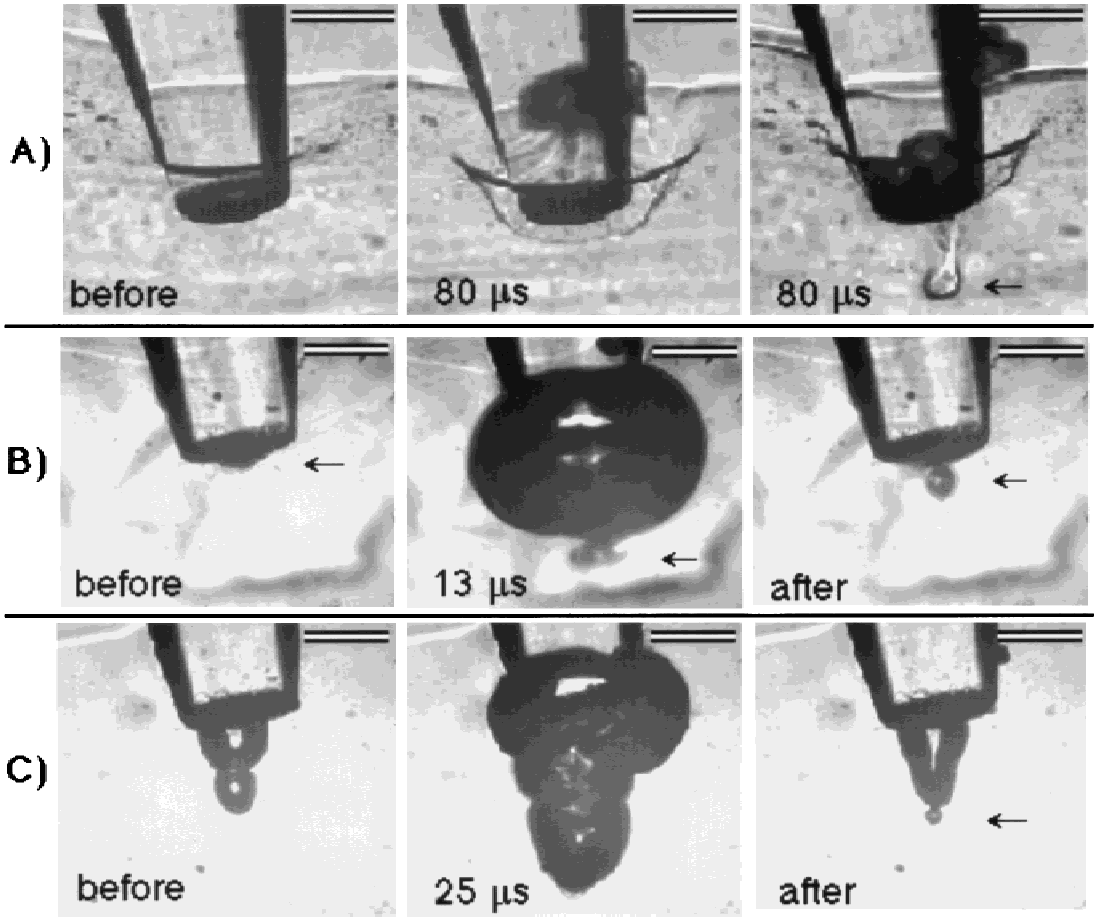

Fig. 4. Micrographs of the cavitation bubble - gel interaction in the presence of an insoluble gas bubble. Length of the bar is 0.25 mm. **A.** Laser energy fluence was 0.35 J/cm^2/pulse, tip exit diameter, 0.24 mm. **Frame 1:** The tip pressing the gel before the first laser pulse. **Frame 2:** The transient socket produced by a cavitation bubble 80 μs after the first excimer laser pulse. Remnants of the collapsing bubble are seen above the sample surface. **Frame 3:** The transient socket 80 μs after the second laser pulse, that was fired when a small gas bubble formed after the first pulse was trapped between the tip and the sample. **B.** Laser energy fluence was 0.3 J/cm^2/pulse, tip exit diameter was 0.33 mm. **Frame 1:** Before irradiation. An arrow indicates a small bubble in front of the tip. **Frame 2:** 13 μs after the excimer laser pulse. An arrow indicates that a small bubble is pushed in front of a large cavitation bubble. **Frame 3:** After the laser pulse. A gas bubble of ~80 μm in diameter is inserted to a depth ~130 μm in front of the tip. **C.** Laser energy fluence was 0.3 J/cm^2/pulse, tip exit diameter was 0.33 mm. **Frame 1:** A two step-shape crater in front of the tip was filled with air before the laser pulse. **Frame 2:** Maximal expansion of the cavitation bubble (25 μs) that inflated the crater with vapor. **Frame 3:** A new step can be seen at the bottom of the crater after the laser pulse.

ated an additional deepening of the crater (Figure 4C, frame 3 in comparison to frame 1). The process of interaction of the cavitation bubble with the gel in the presence of a gas bubble was not reproducible for the first 2–3 pulses, because the appearance, position, and dimension of the insoluble gas bubble changed from pulse to pulse. In contrast, when a pulse train consisting of 4–5 laser pulses was applied to the sample, a deep and narrow crater was always created, similar to the crater shown in Figure 4A, frame 3. Such a behavior was observed with a wide range of repetition rates—between 0.5 to 20 Hz at the energy fluences varying in a range of 0.15–0.35 J/cm^2/pulse.

DISCUSSION

The 193 nm excimer laser is strongly absorbed by biological tissue—it generally has a micron-size penetration depth [17,18]—that results in a low threshold of cavitation bubble formation. For example, in the case of a 20% gelatin gel, this threshold energy fluence is ~60 mJ/cm^2/pulse. Physiological media also absorb this radiation, but much less, so the penetration depth in saline,

e.g., is ~60 μm [15]. This results in the threshold of cavitation bubble formation of ~1.8 J/cm^2/pulse. Energy fluence in vitreoretinal applications generally does not exceed 0.3 J/cm^2/pulse [7], so cavitation bubbles can be created only due to laser absorption in tissue. Separation of the tip from gelatin by 60 μm at an energy fluence of 0.15 J/cm^2/pulse prevents cavitation bubble generation on the surface of gelatin. This is due to both the radiation absorption in saline and the high divergence of the beam at the exit of the tapered tip (0.4 rad). At an energy fluence of 0.3 J/cm^2/pulse, this distance will increase up to ~100 μm. The screening effect of the physiological medium could play an important role in the safe application of this laser. During the surgical procedures of dissection of vitreoretinal membranes, it is not always possible to detect the moment when the membrane has been cut. Thus the surgeon moves the tip gently touching the membrane while firing at a repetition rate of 20–50 Hz until a visible cut is produced. As cavitation bubble formation depends on the absorption coefficient, the excimer laser can "feel the cutting process" and automatically stops the bubble generation when no tissue rests in front of the tip. Thus when a lesion is produced in the membrane located at ~100 μm above the retina, the radiation penetrating through the lesion does not generate cavitation bubbles in the retina. This will not happen with mid-IR lasers such as the pulsed Er:YAG laser, which generates bubbles due to water absorption. In this case bubbles will be formed in the tissue and in the surrounding medium at about the same threshold energies [4,14] since in both cases water molecules are the absorbing entity.

In the case of application of repetitive pulses, insoluble bubbles can be trapped between the tip and the tissue. Such bubbles change the shape of the cavitation bubble (see Fig. 4C, frame 2) and cause deep and narrow craters in the sample (see Fig. 4A, frame 3, B, frame 3). It seems from our observations that the gas bubble trapping efficiency depends on the rigidity of the gel. For example, a decrease of the gelatin content from 20% to 10% makes the gel softer and resulted in better trapping of insoluble bubbles. In addition, the first pulses soften the gel in the irradiated area, and this also makes insoluble bubble trapping easier for the rest of the pulse train. Thus the trapping effect may facilitate the tissue cutting depending on its mechanical properties and the change of these properties during the irradiation.

Craters created in retina by single laser pulses [7] dramatically differ from the craters obtained in gelatin. Even at an energy fluence of 0.35 J/cm^2, no disruption was observed in gelatin after a single pulse application. At this energy fluence, all retinal and chorroidal blood vessels were easily cut by a single laser pulse [7]. Single pulses with an energy fluence of 0.23 and 0.15 J/cm^2 produce in rabbit retina craters of 100 μm and 50 μm in depth, respectively [7]. Therefore, even though gelatin gel is an excellent model for visualization of the cavitation bubble dynamics inside the soft tissue, the mechanical strength of gelatin is much higher than that of retina and thus the resulting craters produced with the same laser pulses are significantly different in these two materials.

CONCLUSIONS

About a 100 μm layer of saline between the laser tip and the tissue is enough to prevent cavitation bubble formation on the tissue surface at the energy fluences applied in vitreoretinal surgery. Small gas bubbles resulting from the laser interaction with the gel and tissue can be confined between the tip and the material. Such confined bubbles influence the next cavitation bubble formation inside the material, and this may result in formation of deep and narrow craters with trains of laser pulses.

REFERENCES

1. Vogel A, Capon M, Asiyo-Vogel M, Birngruber R. Intraocular photodisruption with picosecond and nanosecond laser pulses: Tissue effects in cornea, lens, and retina. Invest Ophthal Vis Sci 1994; 35(7):3032–3044.
2. Vogel A, Schveiger P, Frieser A, Asiyo M, Birngruber R. Intraocular Nd-YAG laser surgery: light-tissue interactions, damage range, and reduction of collateral effects. IEEE J Quantum Electron 1990; 26:2240–2260.
3. Dyer PE, Khosroshahi ME, Tuft SJ. Studies of laser-induced cavitation and tissue ablation in saline using a fiber-delivered pulsed HF laser Appl Phys B 1993; 56: 84–93.
4. Lin C, Stern D, Puliafito C. High-Speed Photography of Er:YAG laser ablation in fluid. Invest Ophthal Vis Sci 1990; 31(12):2546–2550.
5. van Leeuwen TG, van Erven L, Meertence JH, Motamedi M, Post MJ, Borst C. Origin of arterial wall dissections induced by pulsed excimer and mid-infrared laser ablation in the pig. J Am Coll Cardiol 1992; 19:1610–1618.
6. Preisack MB, Neu W, Nyga R, Wehrmann M, Haase KK, Karsch KR. Ultrafast imaging of tissue ablation by a XeCl excimer laser in saline. Lasers Surg Med 1992; 12: 520–527.

7. Palanker D, Hemo I, Turovets I, Zauberman H, Lewis A. Vitreoretinal ablation with the 193 nm excimer laser. Invest Ophthalmol Vis Sci 1994; 35(11):3835–3840.
8. Zysset B, Fujimoto JG, Deutsch TF. Time-resolved measurements of picosecond optical breakdown. Appl Phys B 1989; 48:139–147.
9. Zysset B, Fujimoto JG, Puliafito CA, Birngruber R, Deutsch TF. Picosecond optical breakdown: Tissue effects and reduction of collateral damage. Lasers Surg Med 1989; 9:193–204.
10. van Leeuwen TG, Meertence JH, Velema E, Post MJ, Borst C. Intraluminar vapor bubble induced by excimer laser pulse causes microsecond arterial dilation and invagination leading to extensive wall damage in the rabbit. Circulation 1993; 87:1258–1262.
11. Turovets I, Palanker D, Kokotov Y, Hemo I, Lewis A. Dynamics of cavitation bubble induced by 193 nm ArF excimer laser in concentrated sodium chloride solutions. J Appl Phys 1996; 72(5):2689–2693.
12. Dyer PE, Khosroshahi ME, Tuft SJ. Studies of laser-induced cavitation and tissue ablation in saline using a fiber-delivered pulses HF laser. Appl Phys B 1993; 56: 84–93.
13. Rudhart M, Hirth A. Use of an absorbent in laser lithotripsy with dye laser: In vitro study of fragmentation efficiency and jet formation. J Urol 1994; 152:1005.
14. Jancen ED, Asshauer T, Frenz M, Motamedi M, Delacretaz G, Welch A. Effect of pulse duration of bubble formation and laser-induced pressure waves during holmium laser ablation. Lasers Surg Med 1996; 18:278–293.
15. Turovets I, Palanker D, Lewis A. ArF excimer laser-induced bubble formation during irradiation of NaCl solutions. Photochem Photobiol 1994; 60(5):412–414.
16. A. Veis. "The Macromolecular Chemistry of Gelatin." New York: Academic Press, 1964, p 117.
17. Green H, Boll J, Parrish JA, Kochevar IE, Osseroff AR. Cytoxicity and mutagenicity of low intensity 248 and 193 nm excimer laser radiation in mammalian cells. Cancer Res 1987; 47:410–413.
18. Ediger MN, Pettit GH, Weiblinger RP, Chen CH. Transmission of corneal collagen during ArF excimer laser ablation. Lasers Surg Med 1993; 13:204–210.